Reviewer #3:

Reviewer Report on Manuscript: "Optimizing CCN predictions through inferred modal aerosol composition – a boreal forest case study"

The manuscript provides a thorough and insightful exploration of aerosol-cloud interactions, focusing specifically on cloud condensation nuclei (CCN) closure studies in boreal forest environments. Using a robust, multi-year dataset from SMEAR II (2016–2020), the authors employ forward and inverse modelling approaches to evaluate the impact of size-dependent chemical composition and hygroscopicity on CCN predictions. The study addresses key uncertainties in climate modelling and attempts to constrain modal aerosol composition using CCN observations — an approach with significant scientific merit. The manuscript presents an extensive dataset of ~6,200 concurrent ACSM, CCN and size distribution observations from Hyytiälä, Finland. The manuscript evaluates three methods for predicting CCN concentrations and explores seasonal variability in aerosol hygroscopicity and composition, with a particular focus on the differences between the Aitken and accumulation modes. This work addresses a significant challenge in the field of aerosol-cloud-climate research, particularly in the context of future scenarios involving declining anthropogenic emissions and increased contributions from natural aerosol sources. The authors implement a novel inverse closure technique using optimization to estimate mode-specific κ values. This comprehensive study is highly relevant to the atmospheric sciences community.
The study is well structured, with a clear methodology and appropriate referencing to prior work. However, there are some areas where the clarity could be improved, potential ambiguities could be resolved and minor corrections could be made to enhance the quality of the manuscript. The dataset is extensive and the topic is timely. Nevertheless, clarification or expansion of several methodological and interpretational aspects is required before the manuscript can be considered for publication.

We thank the reviewer for his/her kind attention to the innovative nature of this work and considering it timely. In the revised manuscript we have added more detail on the methods and, in particular, further improved the inverse closure methodology by introducing an approach based on the DREAM-MCMC algorithm, which allows also accounting for the variability of the particle number size distribution during the 2-h long CCN measurement cycle. The results from this more sophisticated approach improve the closure further and corroborate the conclusion on size-dependent hygroscopicity as a key explaining factor for obtaining successful closure. Based on comments and suggestion from other reviewers too, we would like to add few more analysis to the revised manuscript and we have attempted to mention the changes appropriately in this document. Just for clarity, please note that κ_{opt} refers to the method where we use Nelder–Mead optimization, focusing only on the optimization of the modal chemical composition. In the revised manuscript, we have included additional analyses, the most significant of which involves DREAM-MCMC simulations. In this approach, referred to as κ_{MCMC}, we not only optimize the modal chemical composition but also account for the variability of the size-distribution lognormal parameters during the optimization process.

Major Comments
1. The optimization of size-resolved composition is central to this study, yet the method remains a bit opaque. It is not very clear: What parameters are varied during optimization? Are any physical constraints or priors imposed (e.g., known hygroscopicity bounds for organics/inorganics)? Is the optimization performed independently per time point, season, or SS level?

We agree that the methods section was a bit unclear and lacked some details. As also pointed out by other reviewers, we have now revised the text to improve clarity and add more details. For example, we have included new sections: 2.2.3.1, where the Nelder–Mead method is explained in detail and 2.2.3.2, which describes the DREAM-MCMC approach:

"2.2.3.1 Nelder-Mead

The Nelder–Mead simplex algorithm (Gao and Han, 2012) is suitable for both one-dimensional and multidimensional optimization problems and is relatively fast in our application. In our case, we need to optimize only one variable (the fraction of total organic mass in Aitken mode, M_{org1}) and the remaining masses can be derived from it through mass closure constraints. For each time step, the optimization begins with an initial simplex of three trial values of M_{org1}, and the NRMSE is evaluated at each point. The worst-performing value is reflected across the midpoint of the better two to explore whether a more accurate estimate can be found in the opposite direction. If this improves the fit, the algorithm attempts an expansion, pushing further in the same direction. If reflection does not improve the result, a contraction step is taken to move closer to the midpoint. If neither reflection nor contraction improves the outcome, the simplex undergoes shrinkage, tightening around the best-performing solution to focus the search locally. This process continues until the optimization converges, resulting in an estimate of M_{org1} that minimizes the NRMSE between modeled and observed CCN concentrations. Note that Nelder–Mead works well for simple, low-dimensional problems like optimizing just one parameter (e.g., m_{org1}), but it starts to struggle as the number of variables increases and have a tendency for converging to local minima. Hence, in the inverse closure calculations using the Nelder-Mead algorithm we assumed the particle number size distribution and chemical composition to stay constant throughout the CCNc measurement cycle.

2.2.3.2 DREAM-MCMC

In order to assess the importance of the variability of the bimodal size distribution parameters within each CCN cycle, we conduct a second inverse-closure experiment with the number concentration and mean diameter for both modes as additional optimization parameters (simultaneously with M_{org1}). Since optimizing both size distribution parameters and composition introduces a more complex and higher-dimensional parameter space, and we are interested parameter uncertainty, we use a Bayesian inference approach to estimate the parameter posterior distributions. Specifically, we chose the DiffeRential Evolution Adaptive Metropolis Markov Chain Monte Carlo (DREAM-MCMC) algorithm (Vrugt et al. 2009), which has been previously used for inverse CCN-closure studies in idealized cases (Partridge et al. 2012) and is available in the Python PINTS library (Clerx et al. 2019). DREAM-MCMC is an efficient MCMC method (Metropolis et al. 1953, Gelfand et al. 1990) that evaluates multiple Markov chains in parallel and automatically adapts its proposal strategy during sampling, making it particularly efficient for correlated, multi-modal problems such as aerosol-cloud microphysical interactions. To know more about MCMC and Bayesian inference, please see Supplementary note R5.

We initialize the MCMC optimization with Cauchy priors for each parameter, centered on the median values of the fitted bimodal size distributions for each CCN cycle, specifically, the number concentration and geometric mean diameter. For chemical composition we use the median of the ACSM observations during each CCN spectrum cycle. The scale value is the smaller of either 1 (resulting in a Student-*t* distribution) or the median absolute deviation (MAD) of the observations within the given CCN cycle. We constrain the total aerosol mass in each mode to remain within ±10% of the total mass observed by the ACSM and aethalometer.

The priors are truncated to positive values only. We use a heteroskedastic Gaussian likelihood function, such that the highest likelihood is typically where the parameters provide the least squares fit to the CCN observations. The likelihood is defined as

$$L(\theta|\mathrm{Y}) = \prod_{i=1}^{n} \frac{1}{\sqrt{2\pi s_i^2}} exp\left[-\frac{1}{2} s_i^{-2}\left(y_i - \phi(X_i,\theta)\right)^2\right]$$

where s is standard deviation of the noise on each output i, which we assume is 10% of the CCN observations at each supersaturation value. We perform the optimization in a log-transformed parameter space, which improves sampler efficiency by normalizing scale differences between parameters. For each CCN observation window, we run five chains with 40,000 iterations per chain, of which the first 15,000 are used as burn-in/adaptation. Up to two chains are discarded if they deviate strongly in central tendency after burn-in, and the last 20,000 steps of all accepted chains are then used to calculate posterior statistics. Convergence is assessed with the $\hat{R}$-statistic (Gelman and Rubin, 1992), using a relaxed threshold of $\hat{R} < 2.5$ for all five parameters to retain a window in the analysis. The $\hat{R}$-statistic compares the variance within chains to the variance between chains; values close to 1 indicate well-

mixed, converged chains. We use a relaxed threshold because the $\hat{R}$-statistic is quite conservative and because our problem has high correlation between parameters and the potential for multi-modality if there are multiple distinction aerosol populations within one window, which is penalized by the $\hat{R}$-statistic but realistic in this case. Overall, 19% of windows are discarded due to high $\hat{R}$-statistic values. Even with the relaxed threshold, some windows are excluded where the MCMC identifies reasonable parameter values and CCN spectra but the chains fail to mix well and we cannot guarantee the posterior is well explored.

2.2.2 Metrics for assessing variability of lognormal size distribution parameters during CCN cycle

Unlike the Nelder–Mead optimization method, which uses the median of the size distribution during the CCN cycle period, the DREAM-MCMC setup requires the variability of the size distribution as input. To account for this, we calculate the median absolute deviation (MAD) of each lognormal parameter for every CCN cycle observation. The overall distribution of MAD values for the full 5-year dataset is presented in Fig. R5. MAD for individual CCN cycle period is calculated as follow:
Let $I_c = [\, t_c^{start}, t_c^{end})$ be the time window for CCN cycle c; For a given lognormal parameter, k (among geometric mean diameter (GMD), geometric standard deviation (SD) and number concentration in each mode; so total 6 parameters), collect the samples inside this window as $\{x_k\,(t): t \in I_c\} = \{x_{k,1}, x_{k,2}, \ldots, x_{k,n_c}\}$.
Median in the interval is $m_k(c)$:

$$\text{median}\{x_{k,1}, x_{k,2}, \ldots, x_{k,n_c}\}$$

Median Absolute Deviation (MAD) in interval c:

$$\text{median}|x_{k,i} - m_k(c)|, \text{ where } i \text{ varies from 1 to } n_c$$

”

“**Supplementary note R5**
In this section we give a short summary of Bayesian inference and MCMC, then describe the detailed setup of the DREAM-MCMC algorithm used in this study and provide some summary statistics. For a comprehensive review of Bayesian methods, see Gelman et al. (2013). Bayesian inference is a rigorous method for quantifying uncertainty in model parameters, using probability statements. Unknown parameters are treated as random variables with some joint posterior probability distribution, which can be written using Bayes law as:

$$p(\theta|Y) = \frac{p(\theta)L(Y|\theta)}{p(Y)}$$

where $p(\theta)$ is the prior distribution which encompasses what is known about the parameters prior to observing any data, $L(Y|\theta)$ is the likelihood function which measures how well the model fits observed data, and

$$p(Y) = \int p(\theta)p(Y|\theta)\mathrm{d}\theta$$

is the marginal distribution of Y, which represents the probability of observing Y given all possible parameter values θ. The result of conditioning the prior distribution with some observations is the posterior probability distribution $p(\theta|Y)$, which represents the updated probability of the model parameters. Bayesian inference is therefore a process of creating a probability model and iteratively updating that model based on some observations, resulting in a best estimate of the parameters and knowledge about their uncertainty, sensitivity, and correlation (in the case where θ is vector-valued).

Monte Carlo Markov Chain (MCMC) simulations are a methodology for sampling from posterior distributions. Generally, they involve repeatedly and sequentially sampling θ such that each new draw

depends only on the previous sample and therefore forms a Markov chain, and correcting those draws so that the chain converges to the target distribution. Many different algorithms have been proposed for generating and correcting chain samples. Here we use the DiffeRential Evolution Adaptive Metropolis Markov Chain Monte Carlo (DREAM-MCMC) algorithm (Vrugt et al. 2009). This algorithm runs multiple chains simultaneously and adaptively updates the proposal distribution using a randomized subset of the chains' joint history. It also supports large proposal jumps and outlier rejection during the initial burn-in phase, which accelerate convergence. This type of self-adaptive evolutionary strategy is particularly well suited to heavy-tailed or multi-modal posteriors, such as in this study where different combinations of aerosol chemical composition and size distributions parameters could result in similar CCN spectra. "

"**Supplementary note R6**
Figure R5 shows the probability density of median absolute deviation, MAD values fitted with chi-squared distributions for both the Aitken and accumulation modes. The results indicate that the variability is generally small, with distributions strongly centered close to zero and narrow tails. The fitted chi-squared parameters suggest that fluctuations in diameter and sigma are low, whereas number concentrations show comparatively larger spread. Overall, this analysis confirms that the derived parameters remain fairly stable within CCN cycle period, with occasional variability in particle number concentration.

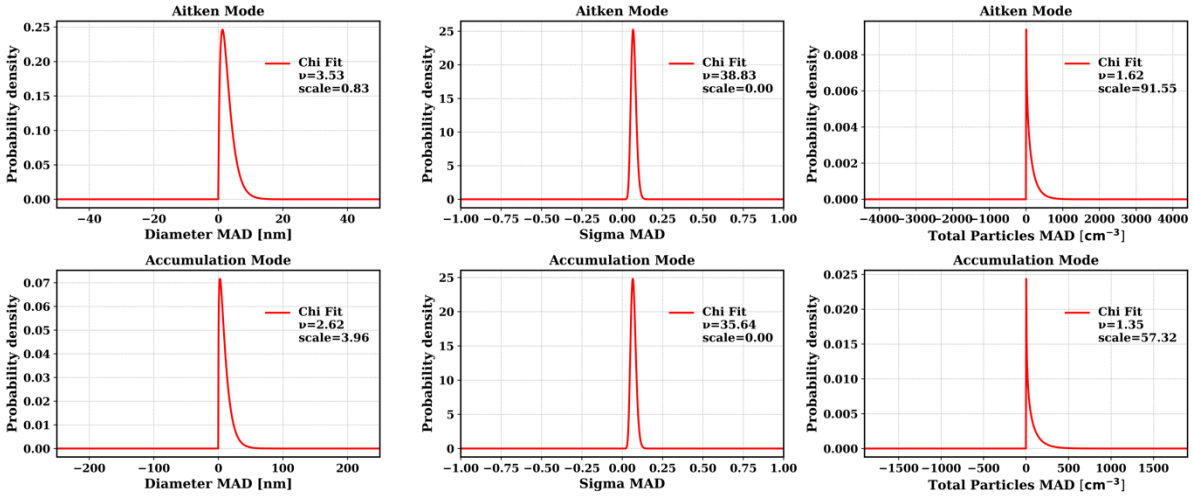

Figure R5. Chi-squared probability density functions (PDFs) fitted to the median absolute deviation (MAD) values of aerosol size distribution parameters calculated with respect to median of corresponding parameters during CCN cycle. The data represent entire 5 years period between 2016 to 2020. Panels show Aitken mode (top row) and accumulation mode (bottom row) MADs for mode diameter, geometric standard deviation (σ), and particle number concentration. The fitted parameters (degrees of freedom, ν, and scale) are reported in the legends. The fits are constrained to non-negative values to reflect the definition of MAD."

We have also added a flowchart (see Fig. R6) to give a clearer overview of the workflow:

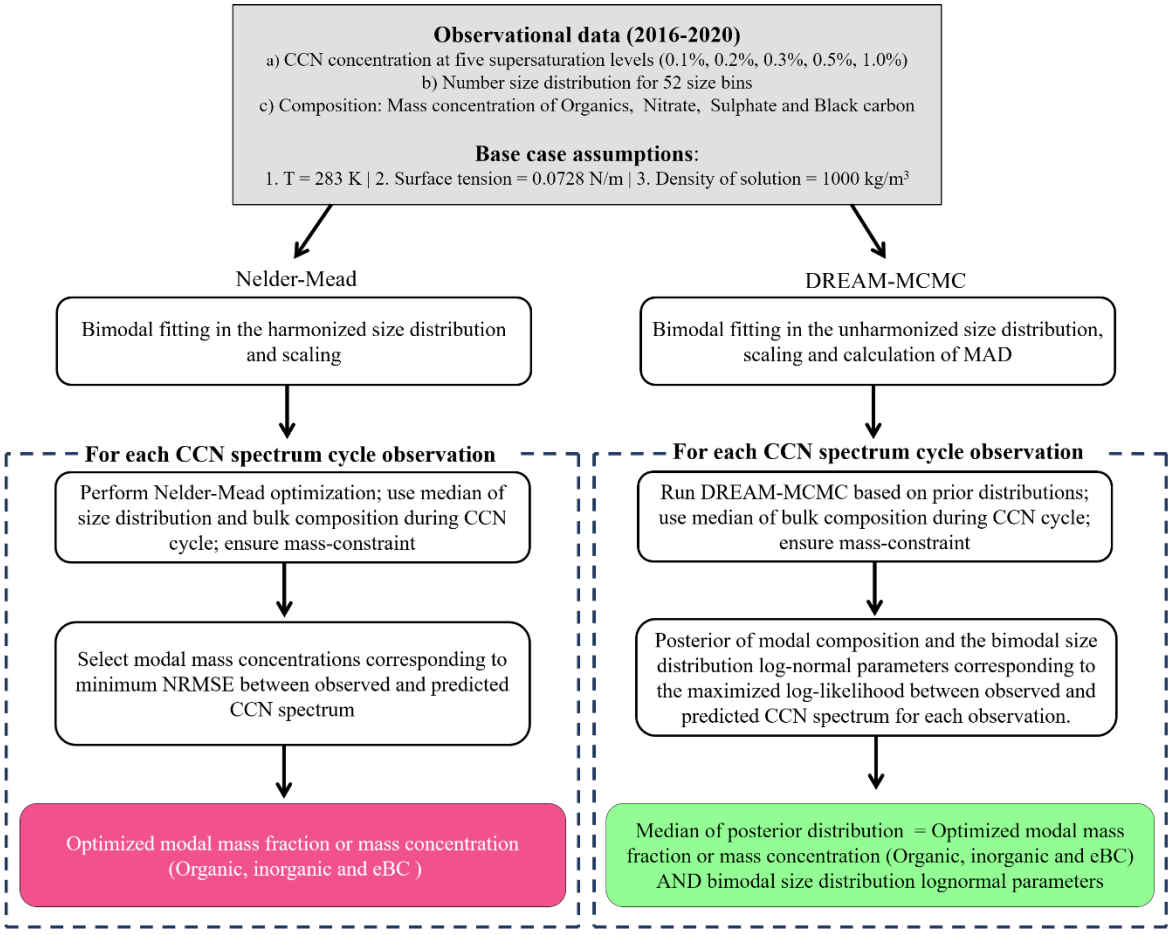

Figure R6. Workflow of the two inverse closure methods: the Nelder–Mead algorithm (left) and the DREAM-MCMC (right) approaches. Bimodal fitting - representation of the aerosol size distribution as two lognormal modes. Harmonized size distribution - size distribution data harmonized to CCN data; data thus obtained has 2-hour resolution. Unharmonized size distribution - raw size distribution data with 10 min resolution. Scaling - adjustment of number concentrations of reconstructed lognormal size distribution from bimodal parameters to match observations. Mass-constraint - conservation of total aerosol mass (sum of mass in two modes) of each species during optimization. NRMSE - normalized root mean square error, a metric of model–observation agreement. MAD - median absolute deviation, used to quantify variability in size distributions during CCN spectrum cycle period. Prior distribution - initial parameter ranges provided to the MCMC sampler. Log-likelihood - statistical measure of consistency between observed and modeled CCN spectra.

2. While the optimized CCN predictions agree better with observations, the inferred composition remains unvalidated. Have the authors compared the mode-specific organic/inorganic fractions with any available independent chemical data (e.g., AMS, offline filters, or PTR-MS)? Without this, there could be a risk of overfitting the CCN closure. Furthermore, the large seasonal variability in composition (e.g., +156% inorganic in winter) should be discussed in the context of known aerosol processes—such as wintertime transport, boundary layer dynamics, or nucleation suppression.

Thanks for this insightful comment. We agree that there is indeed a risk of overfitting if uncertainties in CCN and size distribution measurements are not properly accounted for. These uncertainties alone could explain part of the overprediction when bulk composition is used. However, earlier studies (e.g., Paramonov et al., 2015) have shown significant differences between the hygroscopicity parameters of Aitken and accumulation modes. Since hygroscopicity is strongly linked to chemical composition, this provided the main motivation for our study.

An encouraging outcome is that our approach does not mitigate the overprediction entirely leaving space for further error mitigation when uncertainty in CCN and size distribution measurement are considered. The improvement is especially clear at the highest supersaturations (SS), while at 0.1% SS the improvement is smaller. In that low-SS case, the residual overprediction is likely due more to

instrument-related factors (such as flow rate and low supersaturation conditions) rather than the assumption of bulk vs. size-segregated composition.

3. The improvement is mainly observed above 0.5% supersaturation. The authors should also discuss the implications at low SS and whether the optimization technique could be adapted or constrained to better handle this regime.

Thank you for this insightful comment. In our study, the optimization mainly targets uncertainties in size-resolved chemical composition, which tend to affect CCN activation more at higher supersaturations (SS > 0.5%). This is because the ACSM measurements primarily represent the accumulation mode particles that activates at lower SS (< 0.5%). As a result, CCN predictions based on bulk ACSM composition already match observations quite well in the low-SS regime (except at 0.1%), leaving limited room for further improvement in this regime through composition optimization there. At higher supersaturations, however, the Aitken mode starts to contribute more significantly, and this is where the size-dependence of the hygroscopicity parameter (κ) plays an important role. Our optimization helps to better capture this variability, leading to improved CCN closure above 0.5% SS.

4. The optimization suggests that accumulation mode particles are more enriched in inorganics while the Aitken mode is more organic-richer. This is plausible, but a more mechanistic explanation is needed. For example: Is this pattern consistent with condensation of oxidized VOCs on smaller particles and aqueous-phase processing on larger particles? How does this compare with seasonal biogenic activity or anthropogenic influence? Including a more detailed interpretation supported by prior literature would strengthen the conclusions.

Thank you for raising this important point. As suggested, we have added more recent prior studies (e.g. Lance et al., 2013; Spiteri et al., 2023; Massling et al., 2023) while explaining the observations in the figures. We have added the following discussion (also in relation to the MCMC results added):

"For the optimized CCN spectra (κ_{opt} and κ_{MCMC}), the seasonal probability distributions of the corresponding hygroscopicity parameters for Aitken and accumulation modes are shown in Fig. R7. Both optimization approaches produce almost identical κ distributions for the accumulation mode. In contrast, the Aitken mode exhibits a distinct bimodality in both cases. The Nelder–Mead optimization produces a sharp peak at $\kappa_{\mathrm{Aitken}} \approx 0.1$, whereas the DREAM–MCMC distribution shows a lower but broader peak slightly above 0.1 – which would be in line with the expected hygroscopicities of the BVOC oxidation products present at the measurement site. A secondary peak generally appears between $\kappa_{\mathrm{Aitken}} = 0.5$ and 0.6, with κ_{MCMC} consistently shifted toward the lower end of this range. The exception is winter, where the second peak is more diffuse in both methods. The lower peak in DREAM–MCMC compared to Nelder–Mead reflects differences in how the two methods balance CCN overprediction. Since κ_{bulk} systematically overestimates CCN, the Nelder–Mead optimization compensates by assigning the Aitken mode a much lower hygroscopicity (higher organic fraction). When size-distribution parameters are also allowed to vary, as in κ_{MCMC}, part of this CCN overprediction can instead be explained by variability in size distribution lognormal parameters. Consequently, the smaller κ peak is reduced in height, while the overall distribution remains consistent with the Nelder–Mead method. In general, the probability distribution of Aitken and accumulation mode hygroscopicity parameter from both methods indicates that the Aitken mode can be predominantly organic on a significant number of instances, with most values of κ clustering around typical organic κ of 0.1. This significant difference in hygroscopicity between the two modes exceeds the typical variability in hygroscopicity values observed for various soluble chemical components, suggesting indeed distinct chemical compositions and water uptake properties of the two modes. Overall, in κ_{opt},the variability between seasons is similar for both the Aitken and accumulation mode (see Fig. R9), while in κ_{MCMC} the Aitken mode a significantly higher variability in all seasons. In autumn and winter, the MCMC distributions resemble those from the Nelder-Mead, suggesting a clear organic enrichment in the Aitken mode as compared with the accumulation mode. For the spring and summer however, the distributions of Aitken mode hygroscopicities are more bimodal. The cases where a clear organic enrichment in the

Aitken mode is predicted are generally characterized by relatively high Aitken mode particle number concentrations and large modal diameter – in line with the explanation above.

These results are generally in line with previous studies reporting differences in the hygroscopicity of Aitken and accumulation mode-sized particles (Hämeri et al., 2001; Paramonov et al., 2015). Because the Aitken mode hygroscopicity distributions are bimodal, a single central metric (e.g., the median) can under-represent the distribution. Even so, both approaches reveal some common seasonal patterns: Aitken κ is generally higher in spring and summer and lower in autumn and winter. In the darker seasons, reduced/absent new particle formation (NPF) events and weaker local aerosol production make the accumulation mode more frequently the more hygroscopic mode, while in spring–summer Aitken κ more often approaches or exceeds accumulation values. Accumulation-mode κ remains comparatively stable, typically between 0.2–0.3, with the highest values in winter. This seasonal variability coincides with enhanced summertime photochemistry, which drives new Aitken particle formation from organic vapors and subsequent aging that increases the oxygen-to-carbon ratio of organics, thereby raising their hygroscopicity (Jimenez et al., 2009; Heikkinen et al., 2021).

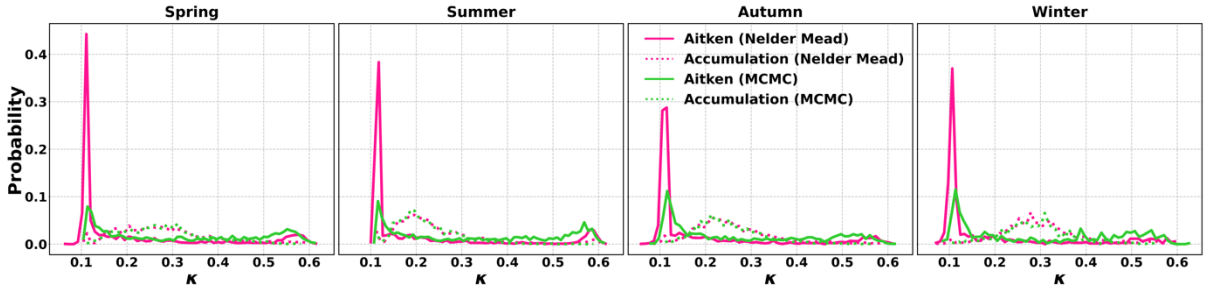

Figure R7. Seasonal probability distributions of the hygroscopicity parameter (κ) for the Aitken and accumulation modes. Each panel corresponds to one season: spring, summer, autumn, and winter. Distributions are shown separately (see legends) for Nelder–Mead optimization and DREAM-MCMC.

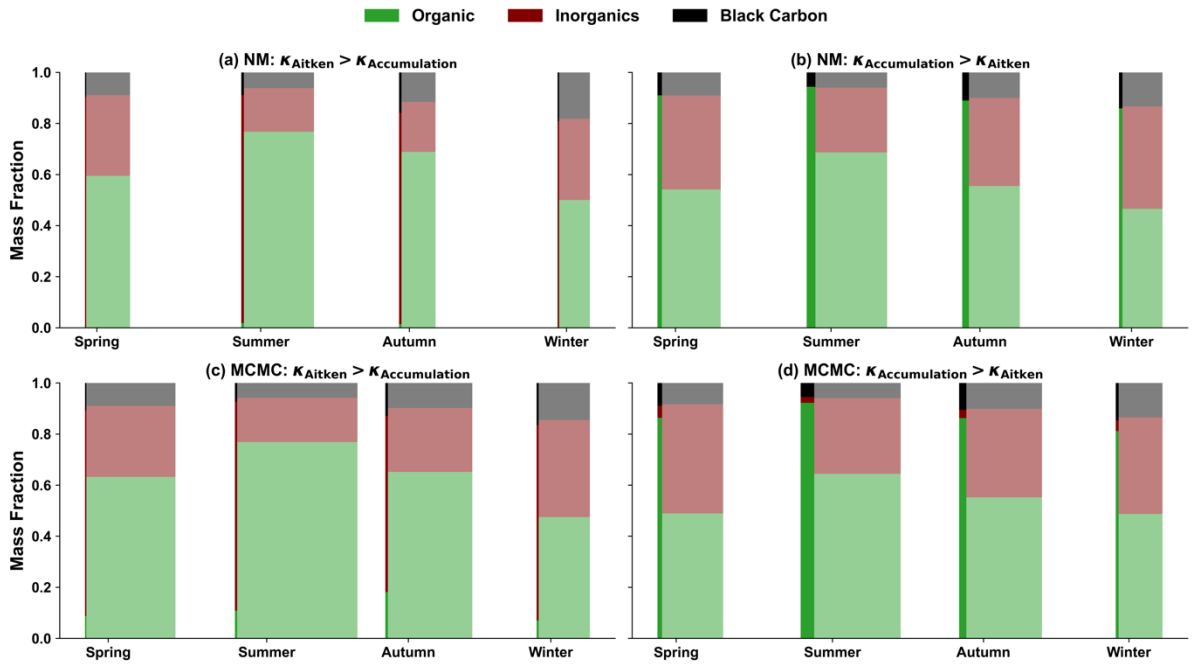

Figure R8. Seasonal mean mass fractions of organic, inorganic, and black carbon components in Aitken and Accumulation modes from Nelder-mead (NM) and DREAM-MCMC optimizations. Panels show cases where $\kappa_{Aitken} > \kappa_{Accumulation}$ (a: NM, c:

MCMC) and $\kappa_{accumulation} > \kappa_{Aitken}$(b: NM, d: MCMC). The stacked bars represent the contributions of organic (green), ammonium sulfate (maroon), and black carbon (black) components within each mode. Aitken mode is depicted with solid colors, while Accumulation mode is represented with slightly faded colors. The width of the bars has been scaled to the mass concentration in the corresponding mode.

Because a bimodal distribution in κ was observed with the MCMC optimization, we separated the optimized data into two groups and examined their size-segregated compositions as presented in Fig. R8. Specifically, we considered cases where $\kappa_{Aitken} > \kappa_{accumulation}$. and cases where $\kappa_{Aitken} < \kappa_{accumulation}$. The mean optimized compositions are shown in Fig. R8, while the corresponding medians are given in Tables S3 (see preprint), S4 (see preprint), R7 and R8. In the Nelder–Mead optimization, $\kappa_{Aitken} > \kappa_{accumulation}$ occurs in 23% of cases, compared to 56% with the MCMC method. Conversely, $\kappa_{Aitken} < \kappa_{accumulation}$ is found in 77% of cases with Nelder–Mead and 46% with MCMC. Despite these differences in frequency, the median κ values shows remarkable agreement between the two approaches. For $\kappa_{Aitken} > \kappa_{accumulation}$, the median GMD_{Aitken}, $GMD_{accumulation}$ (Geometric Mean Diameters), κ_{Aitken}, and $\kappa_{accumulation}$ are 30–32 nm, 133–137 nm, 0.5, and 0.2, respectively. In contrast, for $\kappa_{Aitken} < \kappa_{accumulation}$, they are 37–43 nm, 137–164 nm, 0.1, and 0.27. Thus, cases with higher Aitken κ are characterized by smaller Aitken *GMD* and occurred throughout the year but were much more frequent in summer. This feature has also been reported in previous studies from various environments, where κ increased at diameters typical of Aitken and nucleation mode (particularly below 60 –70 nm) and was often — but not always — associated with new particle formation (NPF) events (Lance et al., 2013; Spiteri et al., 2023; Massling et al., 2023). For $\kappa_{Aitken} > \kappa_{accumulation}$, the Aitken mass is consistently lower than in the $\kappa_{Aitken} < \kappa_{accumulation}$ case (see Fig. R8), reflecting the availability with condensable vapors with low enough volatility to overcome the Kelvin barrier and condense on the Aitken mode. In both optimization methods, the composition patterns within each group are very similar, just as with the κ values (Fig. R7 & R8). For cases where $\kappa_{Aitken} > \kappa_{accumulation}$, the Nelder–Mead predicted the Aitken mode to be almost entirely inorganic, while DREAM-MCMC suggested slightly more organic material but still mostly inorganics. In these cases, both approaches agree that the Aitken mode had the lowest organic fraction in winter and spring. For $\kappa_{Aitken} < \kappa_{accumulation}$, our results, consistent with previous studies at SMEAR II (e.g., Allan et al., 2006), indicate that the accumulation mode contained a larger inorganic fraction, leading to higher hygroscopicity compared to the Aitken mode. Such a difference has also been observed in other similar environments (Timonen et al., 2008; Hao et al., 2013; Levin et al., 2014) as well as in urban Beijing (see also Wu et al., 2016). This disparity in mass fractions of inorganics between the two modes is most pronounced in winter (for example in Nelder-mead optimization, the relative enrichment in Aitken vs. Accumulation model mass fraction being ~156 %) and autumn (the relative enrichment of ~106 %), i.e. the periods when the distinction between Aitken and accumulation modes is most evident (see Fig. 4 in the preprint). This seasonal variation reflects shifts in aerosol sources and processes, and the results are generally in line with what is known. During summer, biogenic SOA is a major source of particulate matter in Hyytiälä (Heikkinen et al., 2021; Yli-Juuti et al., 2022). In contrast, autumn and winter are characterized by a higher mass fraction (and concentration) of inorganic aerosol chemical components (Heikkinen et al., 2020), which highlights the prevalence of transported (Riuttanen et al. 2013) and cloud-processed particles (Isokääntä et al., 2022). Cloud processing leads to both the observed bimodal PNSD (Fig. 3) and a higher sulfate abundance in the accumulation mode (e.g., Leitach et al., 1996; Roelofs et al., 1998; Kreidenweis et al., 2003; Wonaschuetz et al., 2012; Ervens et al., 2018). ”

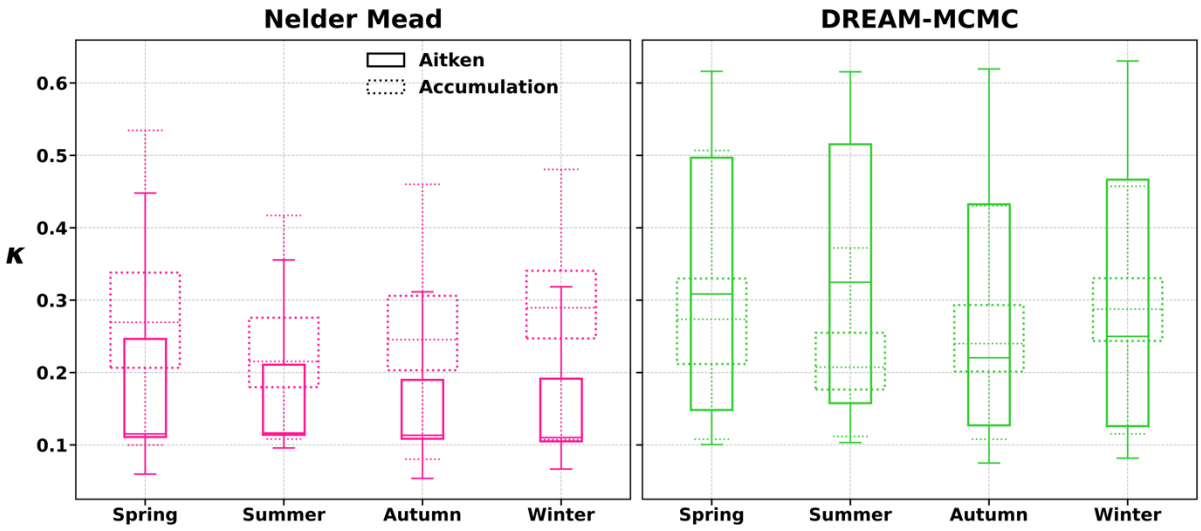

Figure R9. Seasonal variability of κ for Aitken and accumulation mode particles derived using Nelder–Mead optimization (left) and DREAM–MCMC inversion (right). Boxes represent interquartile ranges, whiskers the 5th–95th percentiles, and horizontal lines the medians.

Table R7. Median mass fractions by group and optimization method

Groups	Organics (Aitken)	Inorganics (Aitken)	Black carbon (Aitken)	Organics (Accumulation)	Inorganics (Accumulation)	Black carbon (Accumulation)
$\kappa_{Aitken} > \kappa_{Accumulation}$ (MCMC)	0.11	0.78	0.11	0.69	0.23	0.08
$\kappa_{Aitken} > \kappa_{Accumulation}$ (Nelder-mead)	0.0004	0.87	0.12	0.68	0.23	0.087
$\kappa_{accumulation} > \kappa_{Aitken}$ (MCMC)	0.87	0.04	0.09	0.54	0.37	0.088
$\kappa_{accumulation} > \kappa_{Aitken}$ (Nelder-mead)	0.91	0.0001	0.09	0.09	0.58	0.087

Table R8. Median κ and fraction of data points by group and optimization method

Groups	*Median* κ_{Aitken}	*Median* $\kappa_{accumulation}$	Fraction of data
$\kappa_{Aitken} > \kappa_{Accumulation}$ (MCMC)	0.47	0.21	0.54
$\kappa_{Aitken} > \kappa_{Accumulation}$ (Nelder-mead)	0.50	0.20	0.23
$\kappa_{accumulation} > \kappa_{Aitken}$ (MCMC)	0.13	0.27	0.46
$\kappa_{accumulation} > \kappa_{Aitken}$ (Nelder-mead)	0.11	0.26	0.77

5. While the research questions are outlined at the end of the introduction, the manuscript would benefit from explicitly stating the working hypothesis earlier (perhaps around line 55 or 70). Suggest rephrasing and condensing the goals for better readability and alignment with subsequent methodology.

Thank you for the good suggestion. We have now added the following sentence to the relevant part of the Introduction:

"In this study we intend to use a CCN closure study as a means to infer information on size-dependent chemical composition of CCN-sized aerosol particles, to enhance bulk chemical composition measurements."

6. The inverse modeling framework is a major novelty in this work but is not adequately introduced in terms of assumptions, mathematical implementation, or validation strategies. Clarify what "inverse aerosol-CCN closure" means in practical terms—e.g., optimization method, objective function, constraints used.

Thanks for this suggestion. As discussed in the response to Comment #1 above, we have added substantially more details on the inverse closure methods used to the revised manuscript.

7. The manuscript discusses organic aerosol extensively but does not explain how the complex properties of organics (e.g., surface tension depression, limited solubility) are accounted for in κ parameterization or closure attempts.

Thank you for this observation. In our analysis, the κ parameter is used as an effective hygroscopicity parameter that implicitly accounts for various influences, including limited solubility and possible surface tension effects. However, we do not treat surface tension depression or solubility limitations explicitly. It is worth noting that incorporating surface tension depression into the κ-Köhler framework would typically reduce the activation diameter, leading to higher predicted CCN concentrations. Given that our closure results based on bulk chemical composition already tend to slightly overpredict CCN compared to observations, explicitly accounting for surface tension depression would likely worsen the agreement. To account for this comment (and similar comments from the other reviewers, we have now conducted an inverse closure study testing the sensitivity of the results to the assumptions of organic molecular properties. We performed two types of inverse-closure studies:

a) Using bulk-composition but optimizing only the organic density, ρ_{org} and organic hygroscopicity parameter, κ_{org}
b) Optimizing ρ_{org} and κ_{org} while also accounting for variability of size distribution lognormal parameters

In both tests, κ_{org} was varied between 0.05 and 0.15, while ρ_{org} was varied between 1000 and 3000 kg m^{-3}. Method (a) resulted in a lower NRMSE but suggested a median optimized organic density of 1000 kg m^{-3}, which seems unrealistic. Method (b) produced a slightly higher NRMSE (0.085 compared to 0.079 from κ_{MCMC}) but yielded a more realistic optimized organic density of 2179 kg m^{-3}, with clear seasonal variability (minimum around 1750 kg m^{-3} in summer). This is notably higher than the 1500 kg m^{-3} assumed in the original inverse-closure approach. Both methods produced optimized κ_{org} values between 0.05 and 0.07 depending on the season.

We have described these results (which we feel strengthens our conclusions) in the revised manuscript.

8. There's an implicit assumption that Hyytiälä data can be generalized to other forest regions or clean continental environments. This assumption should be stated explicitly and discussed in the limitations.

Thank you for this great comment. We have now added a sentence stating this assumption ("Through assuming that the SMEAR II station represents a remote continental site with a reasonable accuracy, we aim to provide useful insights on the role and dependencies of natural aerosol on CCN loadings.") to the Introduction and its limitation to the Conclusions ("In the future, the method applied here should be tested at other locations with varying aerosol chemical compositions – also to mitigate the inherent representativity issues related to using data from a single station.") sections of the revised manuscript.

9. The study notes persistent overprediction errors not resolved by optimized κ values. It would strengthen the work to more directly explore model structural assumptions such as: constant surface tension, neglecting semi-volatile partitioning, mixing state (internal mixing assumption for size modes).

Thank you for this excellent comment. Motivated by this suggestion and the suggestions from other reviewers we have now indeed included a more detailed inverse analysis with an additional method (namely the DREAM-MCMC calculation) which allows for letting also the particle number size distribution vary within its uncertainty limits during the CCN measurement cycle. Including the size distribution variability during the CCN measurement cycle improves the closure considerably (see Table R9 and Figs. R10 and R11 below). We have added these figures and their description into the revised manuscript.

Table R9. NRMSEs and Pearson's correlation coefficient (*R* in brackets) corresponding to different methods and supersaturations for all years taken together.

Methods	**NRMSE (*R*) at SS = 0.1%**	**NRMSE (*R*) at SS = 0.2%**	**NRMSE (*R*) at SS = 0.3%**	**NRMSE (*R*) at SS = 0.5%**	**NRMSE (*R*) at SS = 1.0%**
κ_{bulk}	0.94 (0.78)	0.49 (0.85)	0.49 (0.85)	0.59 (0.84)	0.60 (0.79)
$\kappa_{0.18}$	0.71 (0.74)	0.43 (0.84)	0.42 (0.86)	0.50 (0.85)	0.52 (0.81)
κ_{opt}	0.92 (0.78)	0.46 (0.86)	0.43 (0.87)	0.47 (0.88)	0.44 (0.86)
$\kappa_{org} = 0$	0.62 (0.70)	0.49 (0.75)	0.48 (0.77)	0.46 (0.80)	0.47 (0.77)
κ_{MCMC}	0.65 (0.85)	0.17 (0.97)	0.12 (0.99)	0.082 (0.99)	0.045 (0.99)

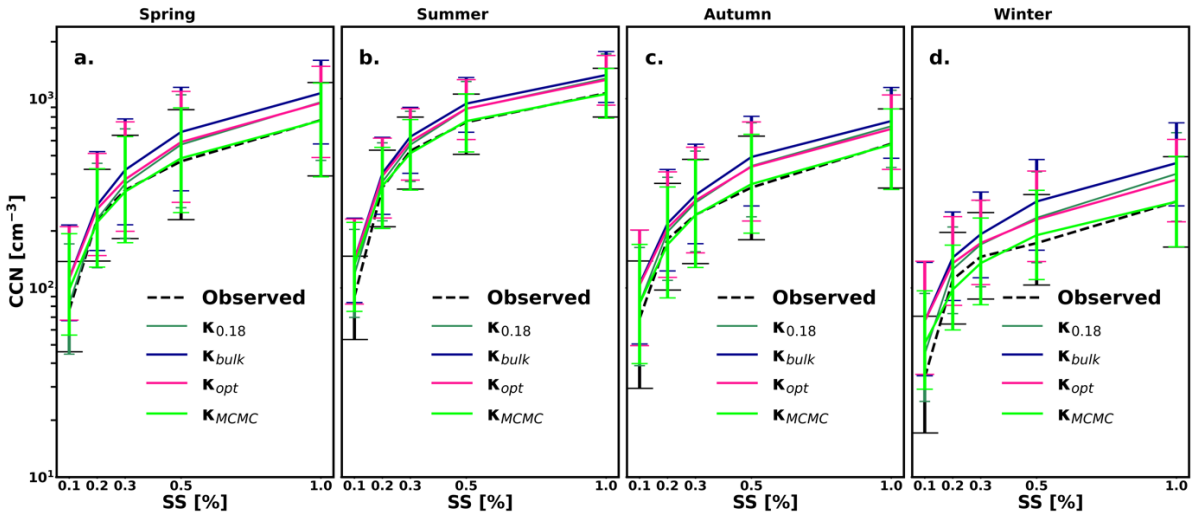

Figure R10. Observed (dashed) and predicted (solid) median CCN spectra in different seasons. The whiskers display the 25th and 75th percentiles.

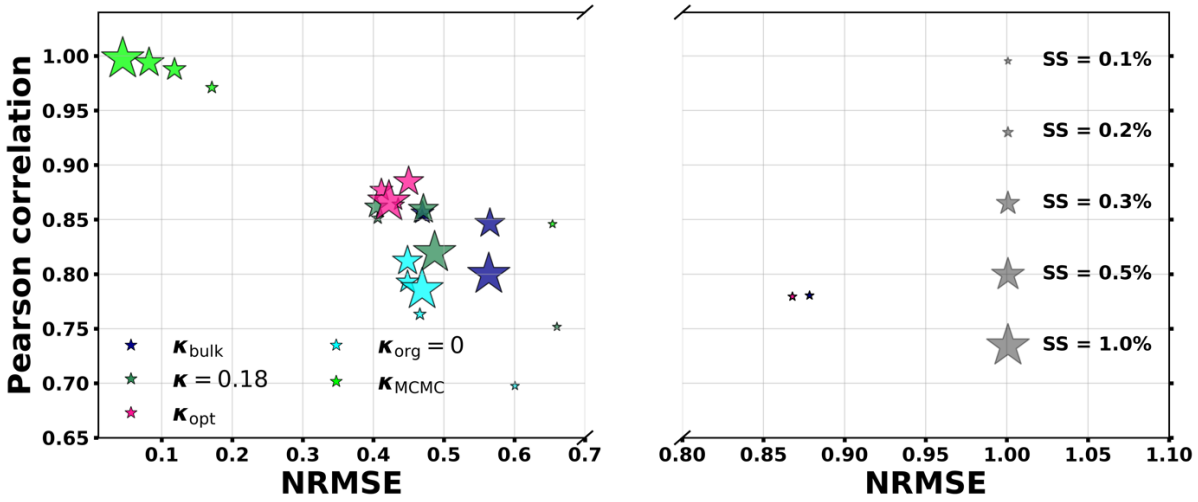

Figure R11. Normalized Root Mean Square Error (NRMSE) and Pearson correlation for different supersaturation (*SS*) levels for all years taken together, comparing four methodologies: κ_{bulk} , $\kappa_{0.18}$, and κ_{opt}, κ_{org}= 0. The two panels split the NRMSE axis to highlight the data in separate ranges, with the left panel covering NRMSE values from 0.3 to 0.6 and the right panel from 0.7 to 1.1. Each point is sized according to the corresponding SS level (0.1%, 0.2%, 0.3%, 0.5%, and 1.0%). The markers are color-coded based on the method for calculating the hygroscopicity parameter, with lines added to represent a discontinuity in the x-axis.

10. The assumption of stable size distributions during the CCN cycle is critical. Was this stability verified using size-resolved time series? Otherwise, this assumption should be treated more cautiously.

Thank you for this excellent comment, see our responses to the comment #9 above. As an outcome of the MCMC calculations included, e.g. the Abstract now reads:

"With reductions in anthropogenic emissions, natural aerosols from boreal forests are expected to play a crucial role in total aerosol loadings. Understanding their cloud-forming potential is therefore crucial. Observational data on aerosol particle number size distribution and chemical composition is required for predicting cloud condensation nuclei (CCN) concentrations using Köhler theory. However, long-term online measurements of bulk chemical composition typically provide data on total sub-micron particulate mass, which only represents the larger end of the number size distribution. Previous studies have shown significant differences in the hygroscopicity of Aitken and accumulation mode particles in boreal environments. Neglecting this size-dependence can substantially overestimate cloud condensation nuclei (CCN) concentrations — particularly at supersaturations (*SS*) where Aitken particles activate. We applied κ-Köhler theory to a multi-year dataset (2016–2020) from Hyytiälä, Finland, to evaluate different representations of aerosol chemical composition for CCN prediction. Forward closure tests using either bulk chemical composition or a constant κ value of 0.18 (Sihto et al., 2011) overpredicted CCN, with geometric mean bias (GMB) highest at *SS* = 0.1% (1.56 and 1.35) and also notable at *SS* = 1.0% (1.34 and 1.26). To mitigate this bias, we performed inverse closure by optimizing size-resolved composition using: (1) Nelder–Mead method with the size distribution fixed to its median during each 2-hour CCN spectrum cycle, and (2) MCMC accounting also for the variability in the particle number size distribution during the CCN measurement cycle. Both methods improved closure at *SS* = 1.0% (GMB = 1.20 and 0.99), with moderate improvement at 0.1%. The optimized results revealed organic enrichment in the Aitken mode in many occasions (as compared with the overall bulk chemical composition): the Aitken mode was enriched in organics in 77% of cases using method (1) and 46% using method (2) – with typical κ values around 0.1 and 0.3 for Aitken and accumulation modes, respectively. The results are generally in line with what is known about size-dependent chemical composition in Hyytiälä, and suggest that most of the variability of aerosol hygroscopicity in Hyytiälä is due to variability in Aitken mode composition. The results also highlight the important role of the highly-variable Aitken mode size distribution in influencing the overall CCN variability at the site. Our results demonstrate the potential of inverse CCN closure methods for

obtaining valuable information of the size-dependent chemical composition beyond the reach of bulk chemical composition measurements."

We have extensively described the new inverse closure results and their description into the revised manuscript.

11. The text mentions calibration frequency for CCNc and invalidation criteria for aethalometer data (e.g., RH > 40%). Please clarify how data gaps or invalid data points were handled in the analysis. Were interpolation or gap-filling methods used? What fraction of data was excluded due to quality control?

Thank you for your comment. For the CCNc data, we did not apply any gap-filling or interpolation methods. Only valid, quality-assured data were used in the analysis. Regarding the equivalent black carbon (eBC) data, approximately 92% of the study period is covered. Data gaps mainly resulted from periods when the instrument was undergoing maintenance or experienced technical issues. As part of our quality control, we excluded data points when the relative humidity inside the aethalometer exceeded 40%, as well as occasional clear outliers. Similar to the CCNc data, no interpolation or gap-filling was performed. All analyses were based solely on available, quality-checked data.

Minor Comments

Line 43: "Aerosol particles are important in the formation…" consider rephrasing as "Aerosol particles play a critical role in the formation…"

Thank you for the suggestion, we have modified the manuscript accordingly.

Line 44: Check the phrasing. Suggest: "...by lowering the energy barrier for the heterogeneous nucleation of water, thus promoting cloud droplet activation…"

Thank you for pointing out this. We have modified the manuscript accordingly.

Line 46-47: Rephrase: "thereby changes in the CCN concentration" to "thus, changes in CCN concentration"

Thank you for pointing out this. We have modified the manuscript accordingly.

Line 57: "drivers of SSmax fluctuations". Define "SS_{max}" explicitly on the first use for clarity.
We have modified the manuscript accordingly.

Line 68: Suggest moving the sentence "These inverse approaches…" earlier to clarify the inverse model's novelty and importance.

We have reworked the respective paragraph for clarity.

Line 93: "Still, organic aerosol plays a significant role…". Consider beginning with "Nevertheless," to better connect to prior sentence.

Thank you for pointing this out. We have modified the manuscript accordingly.

Line 123: Confusing sentence. Suggest: "Specifically, median κ was 0.41 at 0.1% SS (corresponding to larger activation diameters), and 0.14 at 1.0% SS (smaller activation diameters)..."

We have modified the sentence as suggested.

Line 129: Add a clarifying phrase on what "systematic overprediction" means quantitatively.

Systematic overprediction means: when size-independent hygroscopicity parameter was used it produced CCN overprediction in most of the observation with respect to observation at 0.6% and above. We have changed to 'recurring overestimation' for more clarity.

Lines 196-214: The site description is thorough, but additional discussion on how representative the SMEAR II site is for boreal forest aerosols under varying seasonal anthropogenic influence would be valuable.

Thanks for this comment. We believe that the current site description already explains how the sources influencing SMEAR II vary seasonally and how this affects aerosol composition. To improve information in this section, we have now added information on the seasonal fractions of organics, equivalent black carbon, and inorganics, based on the data reported in Heikkinen et al., 2020.

Line 310: "with by a Nafion dryer" to "with a Nafion dryer" (remove "by").

Thanks for the comment. We have implemented it.

Lines 314-315: The ACSM and eBC data are averaged over 1-hour intervals but converted to a 2-hour median to match CCN measurements. Please discuss potential impacts of this temporal averaging on capturing short-term variability in aerosol composition and CCN. Were any tests performed to ensure this does not bias the results?

We did not perform a separate test for this, as the variability of the size distribution was deemed to be the most important source of uncertainty in this regard. The original ACSM data were already averaged to 1 h, since the overall aerosol loading at Hyytiälä is quite low and shorter averaging would not provide meaningful statistics. For comparison with CCN, we further converted these to 2 h medians to match the CCN cycle. This assumes that sub-hourly variability does not strongly influence the calculated κ, as organics—which are relatively less hygroscopic ($\kappa \approx 0.1$) consistently dominate the aerosol composition across seasons. We therefore expect the impact of this temporal averaging on our results to be minimal.

Line 659–661: Consider rephrasing for clarity: "The relative difference in the median Aitken and accumulation κ…" to Perhaps "The seasonal variability in median κ between Aitken and accumulation modes is most pronounced in winter (~162%)..."

Thank you for this comment. We would, however, prefer to keep the sentence as is to keep it clear that the 162% refers to the difference in the Aitken and accumulation mode κ instead of the amplitude of the seasonal variability. We hope this is acceptable.

Line 676–678: Repetition – consider merging: "observed CCN concentrations are a valuable tool… Our study uses this approach…" to avoid redundancy.

Thank you for highlighting this repetition. We have removed the paragraph.

Line 687–688: Suggest citing more recent or diverse κ-related parameterization studies for broader context.

Thank you for the suggestion. We have included a few more studies, such as Lance et al. (2013), Ray et al. (2023), and Siegel et al. (2022).

References

Clerx, M., Robinson, M., Lambert, B., Lei, C. L., Ghosh, S., Mirams, G. R., & Gavaghan, D. J. (2019).

Probabilistic Inference on Noisy Time Series (PINTS). Journal of Open Research Software, 7(1), 23. https://doi.org/10.5334/jors.252

Ervens, B., Sorooshian, A., Aldhaif, A.M., Shingler, T., Crosbie, E., Ziemba, L., Campuzano-Jost, P., Jimenez, J.L., Wisthaler, A., 2018. Is there an aerosol signature of chemical cloud processing? Atmospheric Chemistry and Physics 18, 16099–16119. https://doi.org/10.5194/acp-18-16099-2018

Gelman, A., Shalizi, C.R., 2013. Philosophy and the practice of Bayesian statistics. British Journal of Mathematical and Statistical Psychology 66, 8–38. https://doi.org/10.1111/j.2044-8317.2011.02037.x

Gysel, M., Crosier, J., Topping, D. O., Whitehead, J. D., Bower, K. N., Cubison, M. J., Williams, P. I., Flynn, M. J., McFiggans, G. B., and Coe, H.: Closure study between chemical composition and hygroscopic growth of aerosol particles during TORCH2, Atmos. Chem. Phys., 7, 6131–6144, 2007

Gao, F., Han, L., 2012. Implementing the Nelder-Mead simplex algorithm with adaptive parameters. Comput Optim Appl 51, 259–277. https://doi.org/10.1007/s10589-010-9329-3

Hao, L., Romakkaniemi, S., Kortelainen, A., Jaatinen, A., Portin, H., Miettinen, P., Komppula, M., Leskinen, A., Virtanen, A., Smith, J.N., Sueper, D., Worsnop, D.R., Lehtinen, K.E.J., Laaksonen, A., 2013. Aerosol Chemical Composition in Cloud Events by High Resolution Time-of-Flight Aerosol Mass Spectrometry. Environ. Sci. Technol. 47, 2645–2653. https://doi.org/10.1021/es302889w

Heikkinen, L., Äijälä, M., Daellenbach, K.R., Chen, G., Garmash, O., Aliaga, D., Graeffe, F., Räty, M., Luoma, K., Aalto, P., Kulmala, M., Petäjä, T., Worsnop, D., Ehn, M., 2021. Eight years of sub-micrometre organic aerosol composition data from the boreal forest characterized using a machine-learning approach. Atmospheric Chemistry and Physics 21, 10081–10109. https://doi.org/10.5194/acp-21-10081-2021

Isokääntä, S., Kim, P., Mikkonen, S., Kühn, T., Kokkola, H., Yli-Juuti, T., Heikkinen, L., Luoma, K., Petäjä, T., Kipling, Z., Partridge, D., Virtanen, A., 2022. The effect of clouds and precipitation on the aerosol concentrations and composition in a boreal forest environment. Atmospheric Chemistry and Physics 22, 11823–11843. https://doi.org/10.5194/acp-22-11823-2022

Kreidenweis, S.M., Walcek, C.J., Feingold, G., Gong, W., Jacobson, M.Z., Kim, C.-H., Liu, X., Penner, J.E., Nenes, A., Seinfeld, J.H., 2003. Modification of aerosol mass and size distribution due to aqueous-phase SO2 oxidation in clouds: Comparisons of several models. Journal of Geophysical Research: Atmospheres 108. https://doi.org/10.1029/2002JD002697

Lance, S., Raatikainen, T., Onasch, T. B., Worsnop, D. R., Yu, X.-Y., Alexander, M. L., Stolzenburg, M. R., McMurry, P. H., Smith, J. N., Nenes, A. Aerosol Mixing State, Hygroscopic Growth and Cloud Activation Efficiency during MIRAGE 2006. Atmospheric Chemistry and Physics 2013, 13 (9), 5049–5062. https://doi.org/10.5194/acp-13-5049-2013.

Leaitch, W.R., 1996. Observations Pertaining to the Effect of Chemical Transformation in Cloud on the Anthropogenic Aerosol Size Distribution. Aerosol Science and Technology 25, 157–173. https://doi.org/10.1080/02786829608965388

Levin, E.J.T., Prenni, A.J., Palm, B.B., Day, D.A., Campuzano-Jost, P., Winkler, P.M., Kreidenweis, S.M., DeMott, P.J., Jimenez, J.L., Smith, J.N., 2014. Size-resolved aerosol composition and its link to hygroscopicity at a forested site in Colorado. Atmospheric Chemistry and Physics 14, 2657–2667. https://doi.org/10.5194/acp-14-2657-2014

Liwendahl, M., 2023. The seasonality and inter-annual variation of aerosol particle size distributions in boreal forest. BSc thesis, Department of Environmental Science, Stockholm University.

Massling, A., Lange, R., Pernov, J.B., Gosewinkel, U., Sørensen, L.-L., Skov, H., 2023. Measurement report: High Arctic aerosol hygroscopicity at sub- and supersaturated conditions during spring and summer. Atmospheric Chemistry and Physics 23, 4931–4953. https://doi.org/10.5194/acp-23-4931-2023

Metropolis N, Rosenbluth AW, Rosenbluth MN, Teller AH, Teller E., 1953. Equation of state calculations by fast computing machines. Journal of Chemical Physics 21, 1087-1092.

Paramonov, M., Aalto, P.P., Asmi, A., Prisle, N., Kerminen, V.-M., Kulmala, M., Petäjä, T., 2013. The analysis of size-segregated cloud condensation nuclei counter (CCNC) data and its implications for cloud droplet activation. Atmospheric Chemistry and Physics 13, 10285–10301. https://doi.org/10.5194/acp-13-10285-2013

Paramonov, M., Kerminen, V.-M., Gysel, M., Aalto, P.P., Andreae, M.O., Asmi, E., Baltensperger, U., Bougiatioti, A., Brus, D., Frank, G.P., Good, N., Gunthe, S.S., Hao, L., Irwin, M., Jaatinen, A., Jurányi, Z., King, S.M., Kortelainen, A., Kristensson, A., Lihavainen, H., Kulmala, M., Lohmann, U., Martin, S.T., McFiggans, G., Mihalopoulos, N., Nenes, A., O'Dowd, C.D., Ovadnevaite, J., Petäjä, T., Pöschl, U., Roberts, G.C., Rose, D., Svenningsson, B., Swietlicki, E., Weingartner, E., Whitehead, J., Wiedensohler, A., Wittbom, C., Sierau, B., 2015. A synthesis of cloud condensation nuclei counter (CCNC) measurements within the EUCAARI network. Atmospheric Chemistry and Physics 15, 12211–12229. https://doi.org/10.5194/acp-15-12211-2015

Partridge, D.G., Vrugt, J.A., Tunved, P., Ekman, A.M.L., Struthers, H., Sorooshian, A., 2012. Inverse modelling of cloud-aerosol interactions – Part 2: Sensitivity tests on liquid phase clouds using a Markov chain Monte Carlo based simulation approach. Atmospheric Chemistry and Physics 12, 2823–2847. https://doi.org/10.5194/acp-12-2823-2012

Ray, A., Pandithurai, G., Mukherjee, S., Kumar, V.A., Hazra, A., Patil, R.D., Waghmare, V., 2023. Seasonal variability in size-resolved hygroscopicity of sub-micron aerosols over the Western Ghats, India: Closure and parameterization. Science of The Total Environment 869, 161753. https://doi.org/10.1016/j.scitotenv.2023.161753

Riuttanen, L., Hulkkonen, M., Dal Maso, M., Junninen, H., Kulmala, M., 2013. Trajectory analysis of atmospheric transport of fine particles, SO_2, NO_x and O_3 to the SMEAR II station in Finland in 1996–2008. Atmospheric Chemistry and Physics 13, 2153–2164. https://doi.org/10.5194/acp-13-2153-2013

Roelofs, G.-J. a N., Lelieveld, J., Ganzeveld, L., 1998. Simulation of global sulfate distribution and the influence on effective cloud drop radii with a coupled photochemistry sulfur cycle model. Tellus B 50, 224–242. https://doi.org/10.1034/j.1600-0889.1998.t01-2-00002.x

Siegel, K., Neuberger, A., Karlsson, L., Zieger, P., Mattsson, F., Duplessis, P., Dada, L., Daellenbach, K., Schmale, J., Baccarini, A., Krejci, R., Svenningsson, B., Chang, R.; Ekman, A. M. L., Riipinen, I., Mohr, C. Using Novel Molecular-Level Chemical Composition Observations of High Arctic Organic Aerosol for Predictions of Cloud Condensation Nuclei. Environ. Sci. Technol. 2022, 56 (19), 13888–13899. https://doi.org/10.1021/acs.est.2c02162.

Spitieri, C., Gini, M., Gysel-Beer, M., and Eleftheriadis, K.: Annual cycle of hygroscopic properties and mixing state of the suburban aerosol in Athens, Greece, Atmos. Chem. Phys., 23, 235–249, https://doi.org/10.5194/acp-23-235-2023, 2023.

Timonen, H., Saarikoski, S., Tolonen-Kivimäki, O., Aurela, M., Saarnio, K., Petäjä, T., Aalto, P.P., Kulmala, M., Pakkanen, T., Hillamo, R., 2008. Size distributions, sources and source areas of water-soluble organic carbon in urban background air. Atmospheric Chemistry and Physics 8, 5635–5647. https://doi.org/10.5194/acp-8-5635-2008

Vrugt, J. A., ter Braak, C.J.F., Diks, C.G.H., Robinson, B. A., Hyman, J. M., Higdon, D., 2009. Accelerating Markov Chain Monte Carlo Simulation by Differential Evolution with Self-Adaptive Randomized Subspace Sampling. International Journal of Nonlinear Sciences and Numerical Simulation, 10(3), 273-290. https://doi.org/10.1515/IJNSNS.2009.10.3.273

Wang, J., Cubison, M. J., Aiken, A. C., Jimenez, J. L., Collins, D. R. The Importance of Aerosol Mixing State and Size-Resolved Composition on CCN Concentration and the Variation of the Importance with Atmospheric Aging of Aerosols. Atmospheric Chemistry and Physics 2010, 10 (15), 7267–7283. https://doi.org/10.5194/acp-10-7267-2010.

Wonaschuetz, A., Sorooshian, A., Ervens, B., Chuang, P.Y., Feingold, G., Murphy, S.M., de Gouw, J., Warneke, C., Jonsson, H.H., 2012. Aerosol and gas re-distribution by shallow cumulus clouds: An investigation using airborne measurements. Journal of Geophysical Research: Atmospheres 117. https://doi.org/10.1029/2012JD018089

Wu, Z.J., Zheng, J., Shang, D.J., Du, Z.F., Wu, Y.S., Zeng, L.M., Wiedensohler, A., Hu, M., 2016. Particle hygroscopicity and its link to chemical composition in the urban atmosphere of Beijing, China, during summertime. Atmospheric Chemistry and Physics 16, 1123–1138. https://doi.org/10.5194/acp-16-1123-2016

Yli-Juuti, T., Mielonen, T., Heikkinen, L., Arola, A., Ehn, M., Isokääntä, S., Keskinen, H.-M., Kulmala, M., Laakso, A., Lipponen, A., Luoma, K., Mikkonen, S., Nieminen, T., Paasonen, P., Petäjä, T., Romakkaniemi, S., Tonttila, J., Kokkola, H., Virtanen, A., 2021. Significance of the organic aerosol driven climate feedback in the boreal area. Nat Commun 12, 5637. https://doi.org/10.1038/s41467-021-25850-7